Applied Catalysis B: Environmental 94 (2010) 318–326

Contents lists available at ScienceDirect

Applied Catalysis B: Environmental

journal homepage: www.elsevier.com/locate/apcatb

Modification of Rh/SiO_2 catalyst for the hydrogenolysis of glycerol in water

Yasunori Shinmi [a], Shuichi Koso [a], Takeshi Kubota [b], Yoshinao Nakagawa [a,c], Keiichi Tomishige [a,c,*]

[a] Graduate School of Pure and Applied Sciences, University of Tsukuba, 1-1-1, Tennodai, Tsukuba, Ibaraki 305-8573, Japan
[b] Department of Materials Science, Shimane University, 1060 Nishikawatsu, Matsue 690-8504, Japan
[c] International Center for Materials Nanoarchitectonics Satellite (MANA), National Institute of Materials Science (NIMS) and University of Tsukuba, 1-1-1, Tennodai, Tsukuba, Ibaraki 305-8573, Japan

ARTICLE INFO

Article history:
Received 14 September 2009
Received in revised form 20 October 2009
Accepted 23 November 2009
Available online 14 December 2009

Keywords:
Glycerol
Biomass
Hydrogenolysis
Degradation
Biomass refinery

ABSTRACT

Addition of Re, Mo and W to Rh/SiO_2 enhanced the catalytic activity of the glycerol hydrogenolysis using water as a solvent. The modification with Re gave the highest conversion and yield of 1,3-propanediol (1,3-PrD). The optimized Rh-ReO_x/SiO_2 (Re/Rh = 0.5) catalyst maintained high selectivity to propanediols and suppressed C–C bond breaking even under low H_2 pressure and high reaction temperature, where Rh/SiO_2 is rather active to C–C bond breaking. Characterization results indicate the formation of ReO_x clusters attached to the surface of Rh metal particles. This can cause the synergy between ReO_x and Rh, and the glycerol hydrogenolysis proceeds on the interface between Rh metal surface and attached ReO_x species.

1. Introduction

Much attention has been given to the transformation of biomass and biomass-derived chemicals to fuel and valuable chemicals for the sustainable development [1]. A biorefinery is a facility that integrates the processes of biomass conversion to produce fuel and chemicals [2]. In the biorefinery, glycerol can be regarded as a renewable feedstock because it is the co-product of triglyceride saponification and transesterification with methanol and ethanol to biodiesel fuel from vegetable oils [3]. Transformation of glycerol into valuable chemicals by oxidation, dehydration, dehydroxylation and so on, is promising in the future biorefinery [3]. One of the methods for the glycerol transformation is the conversion to 1,2-propanediol (1,2-PrD) and 1,3-propanediol (1,3-PrD). It has been reported that glycerol was converted to 1,2-propanediol by hydrogenolysis using heterogeneous catalysts [4,5]. In contrast, it has been known that a fermentation method enables the conversion of glycerol to 1,3-propanediol, which is more valuable than 1,2-propanediol, in particular, as a raw material for the production of polyesters [6]. There have been several reports on homogeneous and heterogeneous catalysts for the glycerol hydrogenolysis to 1,3-propanediol. However, in the liquid phase, special solvents are needed: 1-methyl-2-pyrrolidinone for $Rh(CO)_2(acac) + H_2WO_4$ [7], sulfolane for $Rh/C + H_2WO_4$ [8], and 1,3-dimethyl-2-imidazolidinone for $Pt/WO_3/ZrO_2$ [9]. It has been reported recently that Cu-$H_4SiW_{12}O_{40}/SiO_2$ is effective to the catalytic reaction in the gas phase [10]. Since the evaporation of glycerol is energy-consuming, the liquid phase catalytic process will be more suitable. Considering water is a by-product of the glycerol hydrogenolysis, safe, inexpensive water is an ideal solvent. Recently, we have reported that Rh/SiO_2 showed a potential for the glycerol hydrogenolysis in water [11]. This article reports the catalytic performance of the Rh/SiO_2 modified with ReO_x in the glycerol hydrogenolysis and characterization results of the Rh-ReO_x/SiO_2, in particular, in terms of interaction between Rh and Re species.

2. Experimental

2.1. Catalyst preparation

A Rh/SiO_2 catalyst was prepared by impregnating SiO_2 with an aqueous solution of $RhCl_3{\cdot}3H_2O$ (Soekawa Chemical Co., Ltd.). The SiO_2 (G-6, BET surface area 535 m^2/g) was supplied by Fuji Silysia Chemical Ltd. After the impregnation procedure and drying at 383 K for 12 h, they were calcined in air at 773 K for 3 h. Rh-MO_x/SiO_2 (M = Re, Mo, W, Mn, V, Zr) catalysts were prepared by impregnating Rh/SiO_2 after the drying procedure with an aqueous solutions of NH_4ReO_4 (Soekawa Chemical Co., Ltd.), $(NH_4)_6Mo_7O_{24}{\cdot}4H_2O$ (Wako Pure Chemical Industries, Ltd.), $(NH_4)_{10}W_{12}O_{41}{\cdot}5H_2O$ (Wako Pure

* Corresponding author at: Graduate School of Pure and Applied Sciences, University of Tsukuba, 1-1-1, Tennodai, Tsukuba, Ibaraki 305-8573, Japan.
E-mail addresses: tomi@tulip.sannet.ne.jp, tomi@ims.tsukuba.ac.jp (K. Tomishige).

0926-3373/$ – see front matter © 2009 Elsevier B.V. All rights reserved.
doi:10.1016/j.apcatb.2009.11.021

Chemical Industries, Ltd.), $Mn(NO_3)_2{\cdot}6H_2O$ (Wako Pure Chemical Industries, Ltd.), NH_4VO_3 (Wako Pure Chemical Industries, Ltd.), $ZrO(NO_3)_2$ (Wako Pure Chemical Industries, Ltd.). ReO_x/SiO_2 and MoO_x/SiO_2 were also prepared by impregnation SiO_2 with aqueous solution of the same precursors as the case of Rh-ReO_x/SiO_2 and Rh-MoO_x/SiO_2. These were calcined in air 773 K for 3 h after drying at 383 K for 12 h. The loading amount of Rh was 4 wt%, and that of additive was represented by the molar ratio of the additive to Rh. All catalysts were used in powdery form with granule size of <100 mesh.

2.2. Activity test

Catalytic testing was performed in a 190-ml stainless steel autoclave with an inserted glass vessel. An aqueous solution of glycerol or neat glycerol (Wako Pure Chemical Industries, Ltd.) was placed into the autoclaves with a spinner and an appropriate amount of catalysts. After sealing the reactors, their air content was purged by flushing thrice with 1 MPa hydrogen (99.99%; Takachiho Trading Co. Ltd.). Autoclaves were then heated to 393 K and pressurized to 1 MPa for the reduction pretreatment. The temperature was monitored using a thermocouple inserted in the autoclave. After 1 h, the H_2 pressure was increased to 8 MPa at reaction temperature. During the experiment, the stirring rate was fixed at 500 rpm (magnetic stirring). After an appropriate reaction time, the reactors were cooled down and all the gases were collected in a gas bag. The autoclave contents were transformed to vials, and the catalysts were separated by centrifugation and filtration. The standard conditions for the reaction were as follows: 393 K reaction temperature, 8.0 MPa initial hydrogen pressure, 5 h reaction time, 20 mass% glycerol aqueous solution, and 150 mg supported metal catalyst. The parameters were changed appropriately in order to investigate the effect of reaction conditions. Details of the reaction conditions are described in each result. The products were analyzed using a gas chromatograph (Shimadzu GC-2014) equipped with FID. A TC-WAX capillary column (diameter 0.25 mmØ, 30 m) was used for the separation. Products were also identified using GC–MS (QP5050, Shimadzu). The products in the glycerol hydrogenolysis were 1,3-PrD, the most desired one, and 1,2-PrD. The overhydrogenolysis reactions gave 1-propanol (1-PrOH) and 2-propanol (2-PrOH). In addition, the degradation reactions proceeded to give ethylene glycol, ethanol, methanol, and methane. The conversion and the selectivity were defined on the C-based calculated in the same way as reported previously [12]. The mass balance was also confirmed in each result and the difference in mass balance was always in the range of the experimental error. The used catalyst was collected by centrifugation, washed with excess water, and dried in air. A slight loss (<10% in weight) was observed during the recovery process and was compensated with fresh catalyst in each reuse experiment.

Acidity of the catalysts was evaluated by hydrolysis of methyl acetate ($CH_3COOCH_3 + H_2O \rightarrow CH_3COOH + CH_3OH$). The activity of the Rh-ReO_x/SiO_2 catalyst was compared with that of an ion exchange resin of Amberlyst15 (4.7 eq/kg-resin dried; highest operating temperature, 393 K; MP Biomedicals). The reaction was performed in a 190-ml stainless steel autoclave with an inserted glass vessel. In the activity test of Rh-ReO_x/SiO_2 (Re/Rh = 0.5), 150 mg of the catalyst was put into the autoclave together with a spinner and 10 ml of water. After the air content was purged, 1 MPa hydrogen (99.99%; Takachiho Trading Co. Ltd.) was introduced and it was heated to 393 K for the reduction pretreatment. The reactor was cooled down and an appropriate amount of aqueous solution of methyl acetate was added to the autoclave. The final concentration of methyl acetate was adjusted to 5 mass% and the total volume of the aqueous solution was 20 ml. In the activity test Amberlyst15, 6.2 mg of the catalyst, and 20 ml of 5 mass% methyl acetate aqueous solution was placed into the autoclave with a spinner. After purging the reactor, hydrogen (1.0 MPa) was introduced and the temperature was raised to 353 K. After 2 h, the solution was separated from the catalyst and analyzed in a similar way for the activity test of the glycerol hydrogenolysis.

2.3. Catalyst characterization

The surface areas of the catalysts were measured using BET method (N_2 adsorption) with an apparatus (Micromeritics, Gemini). Temperature-programmed reduction (TPR) was carried out in a fix bed reactor equipped with a thermal conductivity detector using 5% H_2 diluted with Ar (30 ml/min). The amount of catalyst was 0.05 g, and temperature was increased from room temperature to 1123 K at the heating rate of 10 K/min. X-ray diffraction (XRD) patterns were recorded by a diffractometer (Philips X'pert). Average metal particle size was estimated using the Scherrer equation [13]. Transmission electron microscope (TEM) images were taken for determination of the particle size (JEOL, JEM 2010). The samples were dispersed in ethanol with supersonic waves and placed on Cu grids under air atmosphere. Average particle size was calculated by $\sum n_i d_i^3 / \sum n_i d_i^2$ (d_i: average particle size, n_i: number of particle with d_i) [14]. The amount of CO chemisorption was measured in a high-vacuum system using a volumetric method. Before adsorption measurements, the catalysts were treated in H_2 at 393 K for 1 h. Subsequently the adsorption was performed at room temperature. Gas pressure at adsorption equilibrium was about 1.1 kPa. The sample weight was about 0.1 g. The dead volume of the apparatus was about 60 cm^3. Adsorption amount of CO is represented as the molar ratio to Rh and this corresponds to the number of the surface atoms assuming that the stoichiometry of adsorbed CO to surface Rh atom is one.

The extended X-ray absorption fine structure (EXAFS) and X-ray adsorption near edge structure (XANES) spectra were measured at the BL01B1 station at SPring-8 with the approval of the Japan Synchrotron Radiation Research Institute (JASRI; proposal no. 2008B1235) and at the NW10A station at Photon Factory at the High Energy Accelerator Research Organization in Tsukuba, Japan (proposal no. 2007G070). The storage ring was operated at 8 and 6.5 GeV, respectively. A Si (1 1 1) single crystal and a Si (3 1 1) single crystal were used to obtain a monochromatic X-ray beam, respectively. Two ion chambers for I_0 and I were filled with 85% N_2 + 15% Ar and 50% N_2 + 50% Ar, respectively, for Re L_3-edge measurement. For Rh K-edge measurement, both ion chambers were filled with Ar.

We prepared the sample after the reduction by pressing 100 and 50 mg of catalyst powder to disk, and the samples gave an edge jump of 0.3 and 0.3 for the Rh K-edge and Re L_3-edge measurement, respectively. The sample disk was pretreated at 393 K with H_2 in a closed circulating vacuum system, and the sample disk was transferred to the measurement cell without exposing to air using a glove box with nitrogen. The sample after the reaction was also prepared. The catalytic reaction was carried out in an autoclave, and the used catalyst powder and the solution were transferred to another measurement cell without exposing air in the grove box. The thickness of the cell filled with the powder was 2 mm to give an edge jump of 0.3 and 0.3 for Rh K-edge and Re L_3-edge measurement, respectively. The EXAFS and XANES data were collected in a transmission mode.

For EXAFS analysis, the oscillation was first extracted from the EXAFS data using a spline smoothing method [15]. Oscillation was normalized by the edge height around 50 eV. Fourier transformation of the k^3-weighted EXAFS oscillation from the k space to the r space was performed to obtain a radial distribution function. The inversely Fourier filtered data were analyzed using a usual curve

fitting method [16,17]. For curve fitting analysis, the empirical phase shift and amplitude functions for the Re–O, Re–Re and Rh–Rh bonds were extracted from data for NH_4ReO_4, Re powder and Rh foil, respectively. Theoretical functions for the Re–Rh and Rh–Re bonds were calculated using the FEFE8.2 program [18]. Analyses of EXAFS data were performed using a computer program (REX2000, ver. 2.5.9; Rigaku Corp.). Error bars for each parameter were estimated by stepping each parameter, while optimizing the others parameter, until the residual factor becomes two times as its minimum value [19]. In the analysis of XANES spectra, the normalized spectra were obtained by subtracting the pre-edge background from the raw data with a modified Victoreen equation and normalizing them by the edge height [20–23].

3. Results and discussion

3.1. Optimization of the additive and its amount

Catalytic performance of modified Rh/SiO_2 catalysts at fixed molar ratio of the additive to Rh (M/Rh = 0.25) in the glycerol hydrogenolysis is compared in Fig. 1. The modification of Rh/SiO_2 with Re, Mo, and W species enhanced the activity of glycerol hydrogenolysis remarkably. In contrast, the modification of Rh/SiO_2 with Mn, V, and Zr species decreased the activity. Similar behavior has been reported in the promoting effect of the modification of Rh with Re and Mo species on the hydrogenolysis of tetrahydrofurfuryl alcohol to 1,5-pentanediol [24,25]. From the result, we investigated the dependence of additive amount over Rh/SiO_2 modified with Re, Mo and W. Fig. 2(a) shows the modification effect of Re. The Re addition enhanced the activity of glycerol hydrogenolysis and the selectivity to 1,3-propanediol (1,3-PrD) simultaneously. The conversion was maximum at Re/Rh = 0.5 with high selectivity to 1,3-PrD, and the optimum amount of Re was determined to be Re/Rh = 0.5. The $Rh\text{-}ReO_x/SiO_2$ (Re/Rh = 0.5) exhibited 22 times higher glycerol conversion and 37 times higher 1,3-PrD yield than Rh/SiO_2. In addition, the degradation reactions were totally suppressed by the modification of Re and the overhydrogenolysis reactions were also suppressed to some extent at the low conversion of glycerol. The amount of CO adsorption on the catalyst is also shown in Fig. 2. The amount of CO adsorption on $Rh\text{-}ReO_x/SiO_2$ catalyst decreased gradually with increasing Re amount. Since the amount of CO adsorption of ReO_x/SiO_2 was zero, CO is adsorbed on the surface Rh atoms. From the comparison between glycerol conversion and the amount of CO adsorption on $Rh\text{-}ReO_x/SiO_2$, the additive effect of ReO_x is not due to the increase of the surface Rh atom but due to the synergy between Rh and Re based on the result that ReO_x/SiO_2 had no activity in glycerol hydrogenolysis [26]. Fig. 2(b) and (c) shows the effect of the Mo and W additive amount. The addition of Mo and W increased the glycerol conversion and the optimum amount was determined to be Mo/Rh = 0.06 and W/Rh = 0.13. The addition of Mo did not influence the selectivity to 1,3-PrD. The addition of W to Rh/SiO_2 enhanced the selectivity to 1,3-PrD, the value of which was almost the same as that for the Re-modified catalyst. From the point of glycerol conversion, the additive effect of Mo and W was not so remarkable as that of Re, though the tendency of the CO adsorption amount is similar. In addition, it has been reported that the addition of H_2WO_4 to $Rh(CO)_2(acac)_2$ [7] and Rh/C [8] in the glycerol hydrogenolysis to 1,3-PrD was effective, and the additive amount ratio was W/Rh = 6.9 and 10, respectively, the values of which were much larger than the present case. This is probably because H_2WO_4 was separated from Rh species in these previous

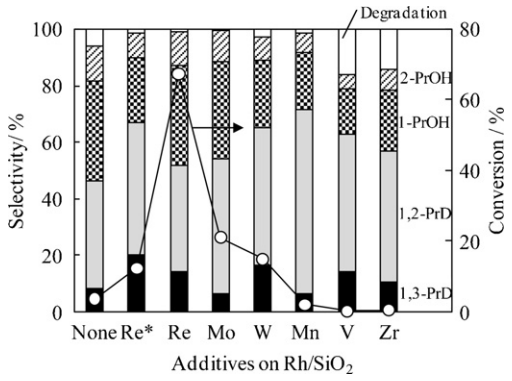

Fig. 1. Comparison of the catalytic the performances in the glycerol hydrogenolysis over modified Rh/SiO_2. Reaction conditions: 20 mass% glycerol aqueous solution 20 ml, reaction temperature 393 K, reaction time 5 h, initial H_2 pressure 8.0 MPa, catalyst 150 mg with the 0.25 molar ratio of additive to Rh. *Re/Rh = 0.5, reaction time 1 h. PrD, propanediol; PrOH, propanol. Degradation: ethylene glycol + ethanol + methanol + methane.

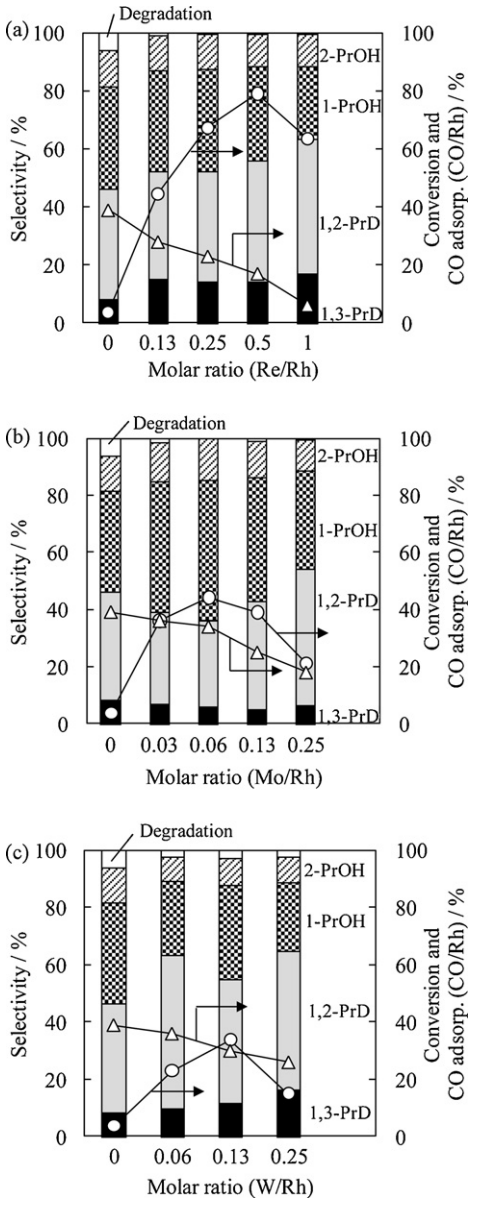

Fig. 2. Dependence of additive amount of Re (a), Mo (b) and W (c) on the glycerol hydrogenolysis over Rh/SiO_2. Open circle: glycerol conversion, open triangle: amount of CO adsorption (CO/Rh). Reaction conditions: 20 mass% glycerol aqueous solution 20 ml, reaction temperature 393 K, reaction time 5 h, initial H_2 pressure 8.0 MPa, catalyst 150 mg. PrD, propanediol; PrOH, propanol. Degradation: ethylene glycol + ethanol + methanol + methane.

reports. On the other hand, the modification method tends to make the direct interaction between the additives and the surface of Rh metal particle [24,25]. The modification of supported Ru catalysts with Re has also been reported to be effective to enhance the activity to glycerol hydrogenolysis. The enhancement (~3 times in conversion of glycerol) correlated with the high dispersion of Ru metal in the modified catalyst [27,28]. On the other hand, the enhancement of glycerol conversion by the modification with Re in our case was much larger (22 times) while the amount of surface Rh atoms in the modified catalyst was decreased by the modification. From the results, it is concluded that the Rh-ReO_x/SiO_2 (Re/Rh = 0.5) was the most effective catalyst, and we focused on this catalyst in the following part of this paper.

3.2. Catalytic performance of Rh-ReO_x/SiO_2 in the glycerol hydrogenolysis

Fig. 3 shows the effect of glycerol concentration over Rh-ReO_x/SiO_2. In this experiment, the total amount of glycerol and water was fixed. The reaction rate of glycerol normalized with the amount of the catalyst was almost unchanged in the solutions of different glycerol concentrations, indicating that the reaction order with respect to glycerol may be zero. It should be noted that hydrogenolysis of neat glycerol without solvents can be catalyzed by the Rh-ReO_x/SiO_2 catalyst.

Fig. 4 shows the effect of H_2 pressure over Rh-ReO_x/SiO_2 (Re/Rh = 0.5) and Rh/SiO_2. On both catalysts, glycerol conversion increased with increasing H_2 pressure. Regarding the selectivity, Rh/SiO_2 tends to give higher selectivity to degradation products at lower H_2 pressure. In contrast, Rh-ReO_x/SiO_2 maintained low selectivity to degradation products even at the lower H_2 pressure, and the effect of H_2 pressure on the selectivity was very small on the Rh-ReO_x/SiO_2. The reaction order of the glycerol hydrogenolysis with respect to H_2 over Rh-ReO_x/SiO_2 was estimated to be first. The result suggests the glycerol hydrogenolysis at low H_2 pressure can be realized on Rh-ReO_x/SiO_2.

Reaction temperature dependence of the glycerol hydrogenolysis over Rh-ReO_x/SiO_2 and Rh/SiO_2 is shown in Fig. 5. Rh/SiO_2 showed higher selectivity to degradation products at higher reaction temperature, though the conversion was as low as 30%. On the other hand, in the case of the Rh-ReO_x/SiO_2 (Re/Rh = 0.5), the selectivity to degradation products was low at even high reaction temperature and high glycerol conversion. An important point is that lower reaction temperature is favorable in terms of the selectivity to 1,3-PrD.

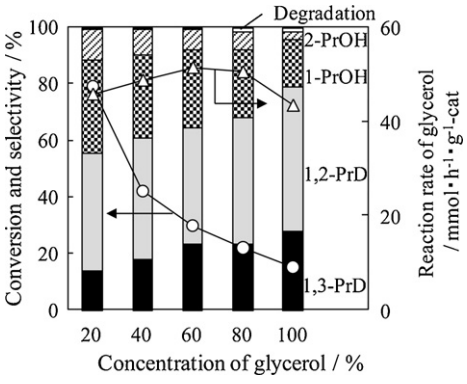

Fig. 3. Effect of glycerol concentration in the glycerol hydrogenolysis over Rh-ReO_x/SiO_2 (Re/Rh = 0.5). Reaction conditions: Glycerol aqueous solution 20 ml or neat glycerol 20 g, reaction temperature 393 K, reaction time 5 h, initial H_2 pressure 8.0 MPa, catalyst 150 mg. PrD, propanediol; PrOH, propanol. Degradation: ethylene glycol + ethanol + methanol + methane.

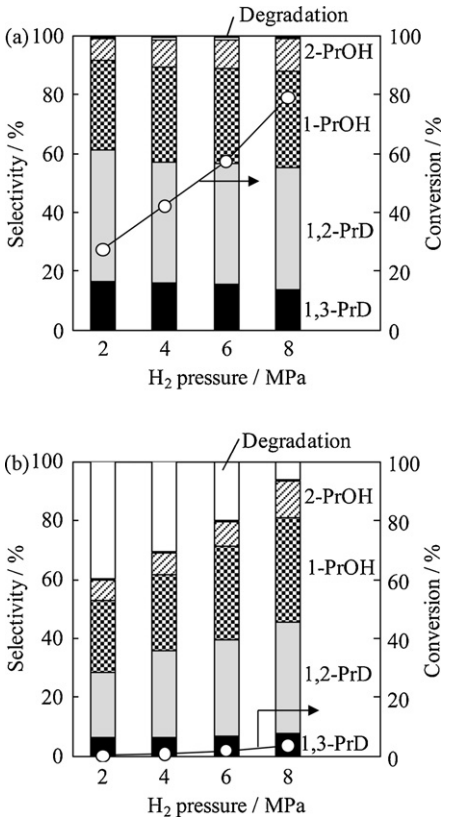

Fig. 4. Effect of H_2 pressure in the glycerol hydrogenolysis over Rh-ReO_x/SiO_2 (Re/Rh = 0.5) (a) and Rh/SiO_2 (b). Reaction conditions: 20 mass% glycerol aqueous solution 20 ml, reaction temperature 393 K, reaction time 5 h, catalyst 150 mg. PrD, propanediol; PrOH, propanol. Degradation: ethylene glycol + ethanol + methanol + methane.

Fig. 6 shows the relation between the glycerol conversion and the selectivity to 1,3-PrD in the glycerol hydrogenolysis over Rh-ReO_x/SiO_2 (Re/Rh = 0.5) under various reaction conditions as shown in Figs. 2–5. As a result, the data of the glycerol conversion and the selectivity to 1,3-PrD are located in a specific region as shown in Fig. 6, and the selectivity to 1,3-PrD tends to decrease with increasing the glycerol conversion. This behavior is related to the consecutive hydrogenolysis of 1,3-PrD. We have reported the hydrogenolysis of 1,2-PrD and 1,3-PrD over Rh-ReO_x/SiO_2 (Re/Rh = 0.5) using 20% aqueous solution of the reactants at 393 K, 2 h, 8 MPa H_2, 0.15 g-cat, where the reaction conditions are similar to those in Fig. 5(a) [26]. The conversions hydrogenolysis in glycerol, 1,3-PrD and 1,2-PrD were 38.4%, 11.8% and 14.0%, respectively [26]. Based on the results, the consecutive hydrogenolysis of 1,3-PrD in the glycerol hydrogenolysis can decrease the selectivity to 1,3-PrD more significantly when the glycerol conversion become higher. Therefore, the yield of 1,3-PrD in the hydrogenolysis of glycerol aqueous solution and neat glycerol was limited to be about 10%. In order to improve the yield of 1,3-PrD, it is necessary to enhance the selectivity to 1,3-PrD from glycerol and to suppress the consecutive hydrogenolysis of 1,3-PrD.

Fig. 7 shows the results of the reuse of Rh-ReO_x/SiO_2 (Re/Rh = 0.5). The glycerol conversion decreased gradually by the repetition, however the selectivity was maintained. One possible reason for this small deactivation is the leaching of small amount of Re as reported previously [24]. Further investigation is necessary in order to clarify the deactivation mechanism.

Fig. 8 shows the effect of solvents on the glycerol hydrogenolysis over Rh-ReO_x/SiO_2 (Re/Rh = 0.5). Alcohols such as methanol, ethanol, and 1-butanol are not effective. In addition,

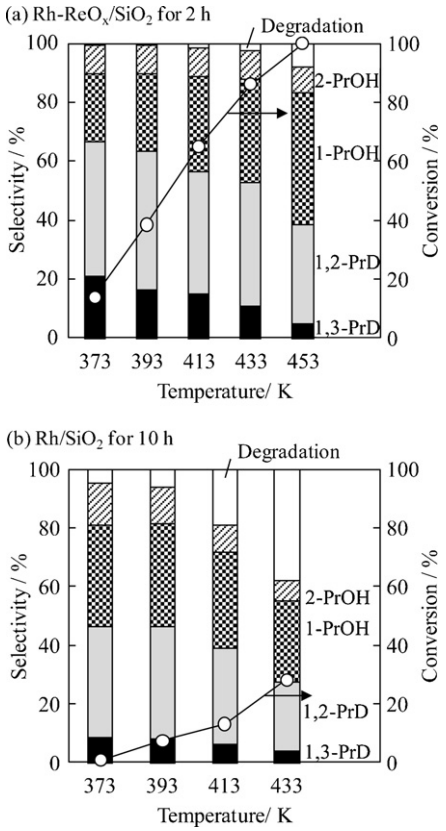

Fig. 5. Reaction temperature dependence of the glycerol hydrogenolysis over Rh-ReO_x/SiO_2 (Re/Rh = 0.5) (a) and Rh/SiO_2 (b). Reaction conditions: 20 mass% glycerol aqueous solution 20 ml, reaction time 2 h for Rh-ReO_x/SiO_2, 10 h for Rh/SiO_2, initial H_2 pressure 8.0 MPa, catalyst 150 mg. PrD, propanediol; PrOH, propanol. Degradation: ethylene glycol + ethanol + methanol + methane.

when 1-methyl-2-pyrrolidinone [7] and sulfolane [8] were used as a solvent, the hydrogenolysis of glycerol over Rh-ReO_x/SiO_2 was suppressed more strongly, though the details are not shown here. As a result, it is found that H_2O is a good solvent for the glycerol hydrogenolysis over Rh-ReO_x/SiO_2. Considering H_2O is a by-product of the glycerol hydrogenolysis, this property is promising. On the basis of the result that the presence of alcohols suppressed the hydrogenolysis of glycerol, 1- and 2-propanols may not be suitable solvents, though they are also by-products of the glycerol hydrogenolysis.

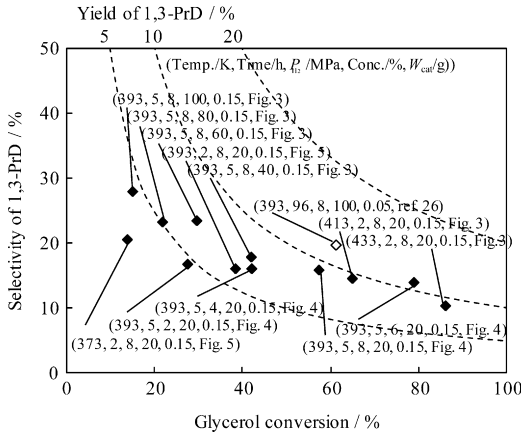

Fig. 6. Relation between the glycerol conversion and the selectivity to 1,3-PrD in the glycerol hydrogenolysis over Rh-ReO_x/SiO_2 (Re/Rh = 0.5).

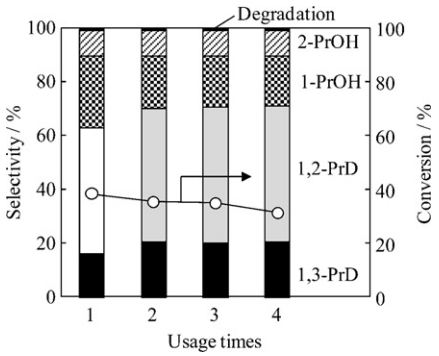

Fig. 7. Reuse of Rh-ReO_x/SiO_2 (Re/Rh = 0.5) in the glycerol hydrogenolysis. Reaction conditions: 20 mass% glycerol aqueous solution 20 ml, reaction temperature 393 K, reaction time 2 h, initial H_2 pressure 8.0 MPa, catalyst 150 mg. PrD, propanediol; PrOH, propanol. Degradation: ethylene glycol + ethanol + methanol + methane.

3.3. Catalyst characterization

Fig. 9(a) shows XRD patterns of the Rh-ReO_x/SiO_2 catalyst after the reduction and the reaction. The peak around $2\theta = 41^\circ$ is assigned to Rh metal, and the average size of Rh metal particles was estimated to be 3.1 ± 0.3 nm. The size was maintained after the reaction. Another important point is that the peak due to Re species was not detected, suggesting that the Re species is highly dispersed. Fig. 9(b) shows the TEM images of Rh-ReO_x/SiO_2 (Re/Rh = 0.5) after the reaction. The particles observed in the TEM can be assigned to the Rh metal particle. The average particle size was calculated to be 2.9 ± 0.2 nm, which agreed well with the particle size obtained from the XRD pattern.

The profiles of temperature-programmed reduction (TPR) of Rh/SiO_2, ReO_x/SiO_2 and Rh-ReO_x/SiO_2 after the calcination at 773 K are shown in Fig. 10. In the case of Rh/SiO_2 containing 0.39 mmol Rh/g-cat, the H_2 consumption peak was observed at 350 K and the amount of H_2 consumption was 0.56 mmol/g-cat, which agreed with the stoichiometry of the reduction of Rh_2O_3 ($Rh_2O_3 + 3H_2 \rightarrow 2Rh + 3H_2O$). The peak of ReO_x/SiO_2 containing 0.19 mmol Re/g-cat was observed at much higher temperature, and H_2 consumption amount was 0.26 mmol/g-cat H_2. This consumption suggests that the Re is reduced from +7 to +4 on the basis that Re species is present as +7 after the calcination as shown later from the XANES and EXAFS results. On the other hand, the Rh-ReO_x/SiO_2 (Re/Rh = 0.5) gave the peak at 370 K, and the H_2 consumption amount was determined to be 0.99 mmol/g-cat. The difference in the H_2 consumption amount between Rh-ReO_x/SiO_2

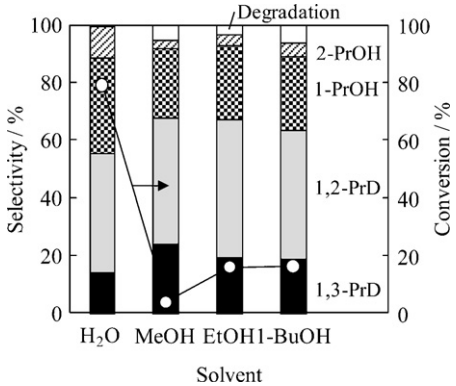

Fig. 8. Effect of solvent on the catalytic performance of the glycerol hydrogenolysis over Rh-ReO_x/SiO_2 (Re/Rh = 0.5). Reaction conditions: 20 mass% glycerol aqueous solution 20 ml, reaction time 5 h, initial H_2 pressure 8.0 MPa, catalyst 150 mg. PrD, propanediol; PrOH, propanol; MeOH, methanol; EtOH, ethanol, BuOH, buthanol. Degradation: ($C_1 + C_2$) excluding solvents.

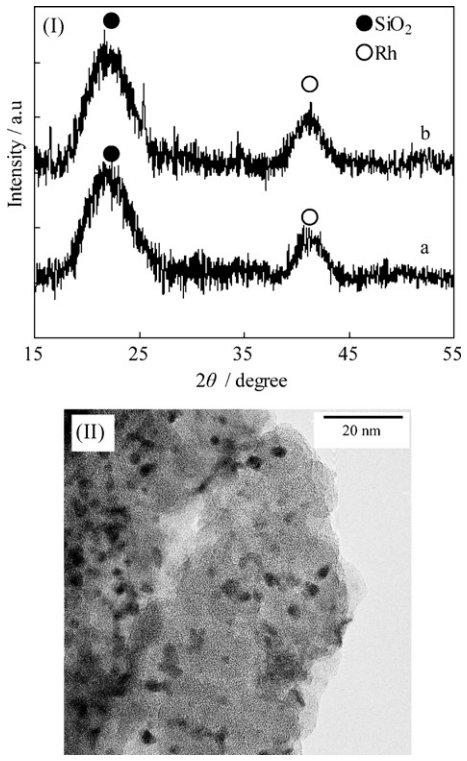

Fig. 9. I. XRD patterns of Rh-ReO_x/SiO_2 (Re/Rh = 0.5) after the reduction (a) and the catalytic use (b). II. TEM image of Rh-ReO_x/SiO_2 (Re/Rh = 0.5) after the catalytic use.

(0.99 mmol/g-cat) and Rh/SiO_2 (0.56 mmol/g-cat) is due to the reduction of Re species on Rh-ReO_x/SiO_2, which was larger than that on ReO_x/SiO_2 (0.26 mmol/g-cat). This result indicates that the presence of Rh promoted the reduction of Re species.

Fig. 11 shows the Re L_3-XANES spectra of Rh-ReO_x/SiO_2 and reference compounds, and the relation between white line area and valence of Re. The first peak in the L_3-edge XANES is called as a white line, and the white line area in the L_3-edge XANES is known to be an informative indication of the electronic state. The larger white line intensity is due to greater electron vacancy in *d*-orbital. As reported previously, a relative electron deficiency and ionic valence can be determined on the basis of the white line intensity [20–23]. Regarding the reference compounds, ionic valence of Re species is almost proportional to the white line intensity. Therefore, the average value of Re species can be estimated by examining the white line area in the XANES spectra [29,30]. The ionic valence of Re species on Rh-ReO_x/SiO_2 (Re/Rh = 0.5) can be determined by the relation between the ionic valence and the

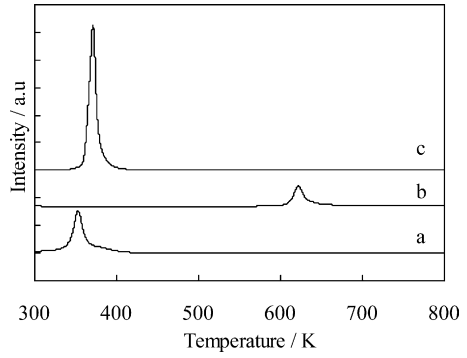

Fig. 10. TPR profiles of the Rh/SiO_2 (a), ReO_x/SiO_2 (b) and Rh-ReO_x/SiO_2 (Re/Rh = 0.5) (c). The Re loading amount of ReO_x/SiO_2 was the same as that of Rh-ReO_x/SiO_2 (Re/Rh = 0.5).

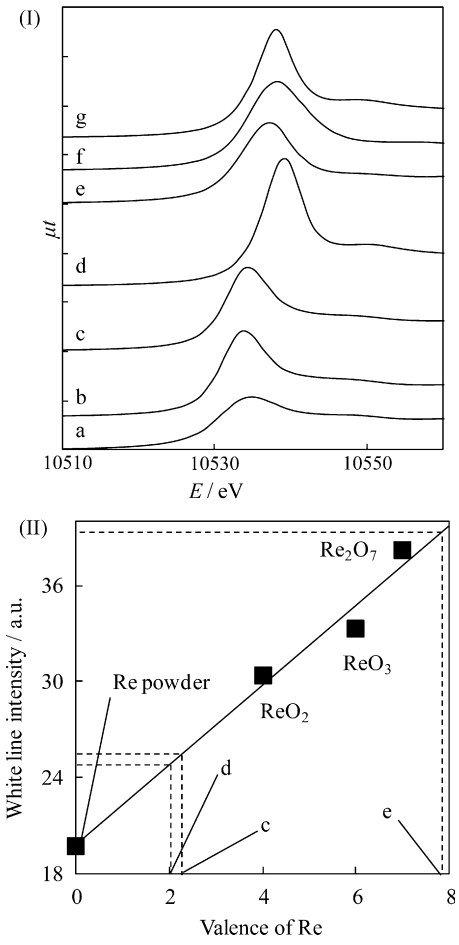

Fig. 11. Results of Re L_3-edge XANES analysis of Rh-ReO_x/SiO_2 (Re/Rh = 0.5). I. Re L_3-edge XANES spectra. II. Relation between white line area and valence of Re. (a) Re powder, (b) Rh-ReO_x/SiO_2 (Re/Rh = 0.5) after the catalytic use, (c) Rh-ReO_x/SiO_2 (Re/Rh = 0.5) after the reduction, (d) Rh-ReO_x/SiO_2 (Re/Rh = 0.5) after the calcination, (e) ReO_2, (f) ReO_3, (g) Re_2O_7.

white line intensity of the reference compounds. The average valence of the Re species on calcined Rh-ReO_x/SiO_2 was determined to be +7, which was the same as that of Re precursor. In the case of Rh-ReO_x/SiO_2 after the reduction and the reaction, the average valence was determined to be +2.2 and +2.0, respectively. The TPR profile of Rh-ReO_x/SiO_2 (Re/Rh = 0.5) indicates that Re species is reduced to +2.5 (Fig. 10). The difference in the valence from between the XANES analysis and TPR can be explained by the difference of H_2 pressure of TPR (0.05 atm) from that for H_2 pretreatment in XANES/EXAFS measurement (1 atm) and for the reaction (8 MPa).

In order to characterize the interaction of Re species with Rh metal particles, Re L_3-edge and Rh *K*-edge EXAFS analyses were carried out. Fig. 12 shows the Re L_3-edge EXAFS spectra of Rh-ReO_x/SiO_2 (Re/Rh = 0.5) after the calcination, reduction and reaction. Table 1 summarizes the curve fitting results. In the case of the calcined Rh-ReO_x/SiO_2 (Re/Rh = 0.5), the FT spectrum was similar to that of NH_4ReO_4, and the curve fitting indicates the presence of the Re–O bond with the coordination number of 4.0 ± 1.0. It is suggested that the Re species can be present as ReO_4^-, and the interaction of ReO_4^- with Rh metal particles detected by XRD was not recognized. The spectrum of Rh-ReO_x/SiO_2 (Re/Rh = 0.5) was drastically changed by the reduction pretreatment and it was almost maintained during the reaction. The curve fitting analysis indicates the presence of the Re–O, Re–Rh and Re–Re bond. The presence of the Re–O bond indicates that Re species is not fully reduced to metallic

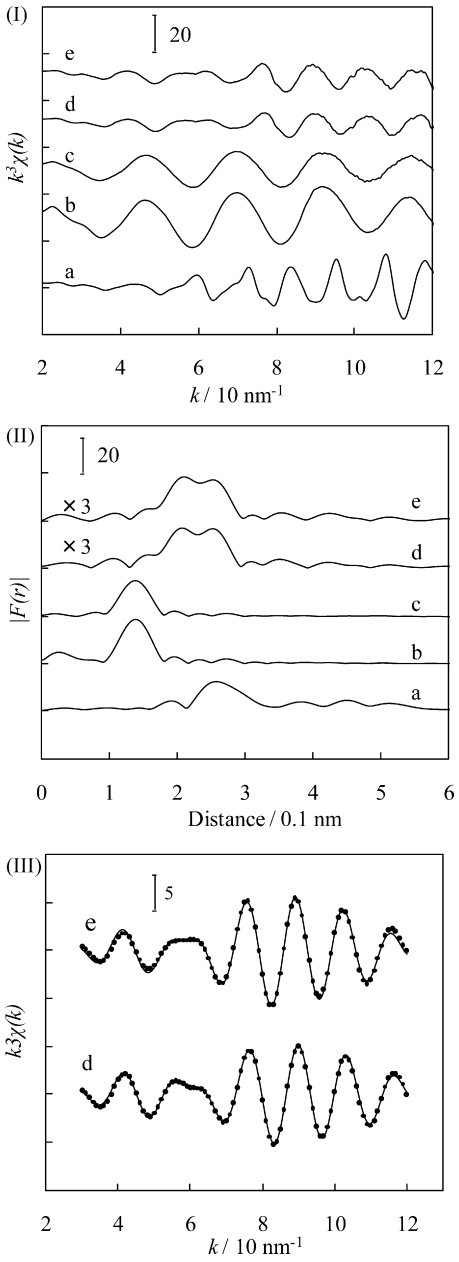

Fig. 12. Results of Re L_3-edge EXAFS analysis of Rh-ReO_x/SiO_2. I. k^3-weighted EXAFS oscillations. II. Fourier transform of k^3-weighted Re L_3-edge EXAFS, FT range: 30–120 nm^{-1}. III. Fourier filtered EXAFS data (solid line) and calculated data (dotted line), Fourier filtering range: 0.129–0.301 nm. (a) Re powder, (b) NH_4ReO_4, (c) Rh-ReO_x/SiO_2 (Re/Rh = 0.5) after the calcination, (d) Rh-ReO_x/SiO_2 (Re/Rh = 0.5) after the reduction, (e) Rh-ReO_x/SiO_2 (Re/Rh = 0.5) after the catalytic use.

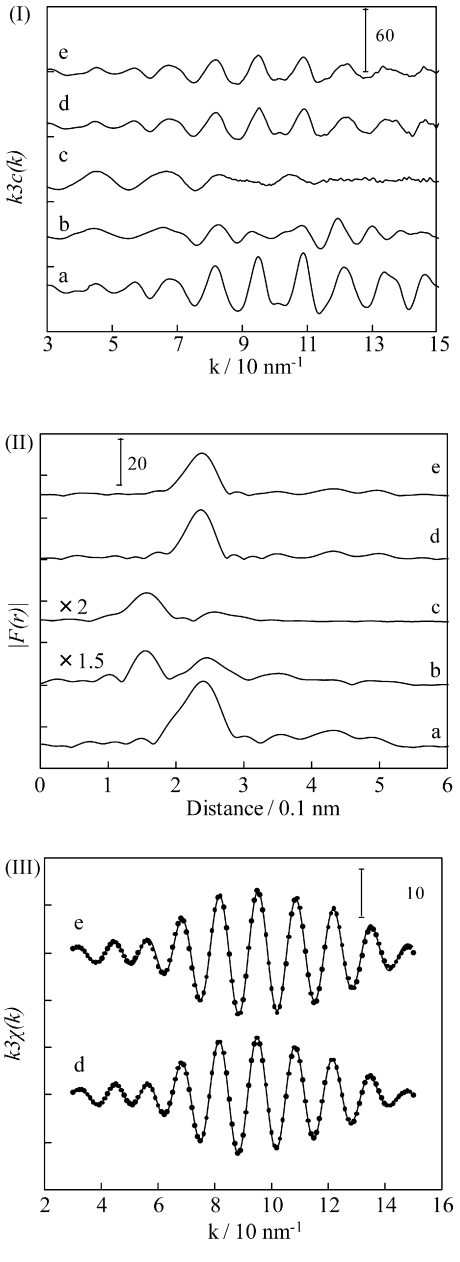

Fig. 13. Results of Rh K-edge EXAFS analysis of Rh-ReO_x/SiO_2 (Re/Rh = 0.5). I. k^3-weighted EXAFS oscillations. II. Fourier transform of k^3-weighted Rh K-edge EXAFS, FT range: 30–150 nm^{-1} (after the reduction and the catalytic use), and 30–120 nm^{-1} (after the calcination). III. Fourier filtered EXAFS data (solid line) and calculated data (dotted line), Fourier filtering range (before and after reaction): 0.153–0.304 nm. (a) Rh foil, (b) Rh_2O_3, (c) Rh-ReO_x/SiO_2 (Re/Rh = 0.5) after the calcination, (d) Rh-ReO_x/SiO_2 (Re/Rh = 0.5) after the reduction, (e) Rh-ReO_x/SiO_2 (Re/Rh = 0.5) after the catalytic use.

Table 1
Curve fitting results of Re L_3-edge EXAFS of Rh-ReO_x/SiO_2 (Re/Rh = 0.5).

Catalyst	Pretreatment	Shells	CN[a]	R (10^{-1} nm)[b]	σ (10^{-1} nm)[c]	ΔE_0 (eV)[d]	R_f (%)[e]
Rh-ReO_x/SiO_2	Calcination	Re-O	4.0	1.74	0.064	0.2	1.6
	Reduction	Re-Rh	3.7	2.65	0.073	10.9	1.1
		Re-Re	2.7	2.72	0.076	3.8	
		Re-O	1.4	2.10	0.093	10.9	
	Catalytic use	Re-Rh	3.7	2.66	0.071	10.5	0.8
		Re-Re	2.8	2.73	0.065	7.4	
		Re-O	1.4	2.11	0.086	10.7	

[a] Coodination number.
[b] Bond distance.
[c] Debye–Waller factor.
[d] Difference in the origin of photoelectron energy between the reference and the sample.
[e] Residual factor. Rh: 4 wt%, Re/Rh = 0.5. Fourier filtering range: 0.129–0.301 nm.

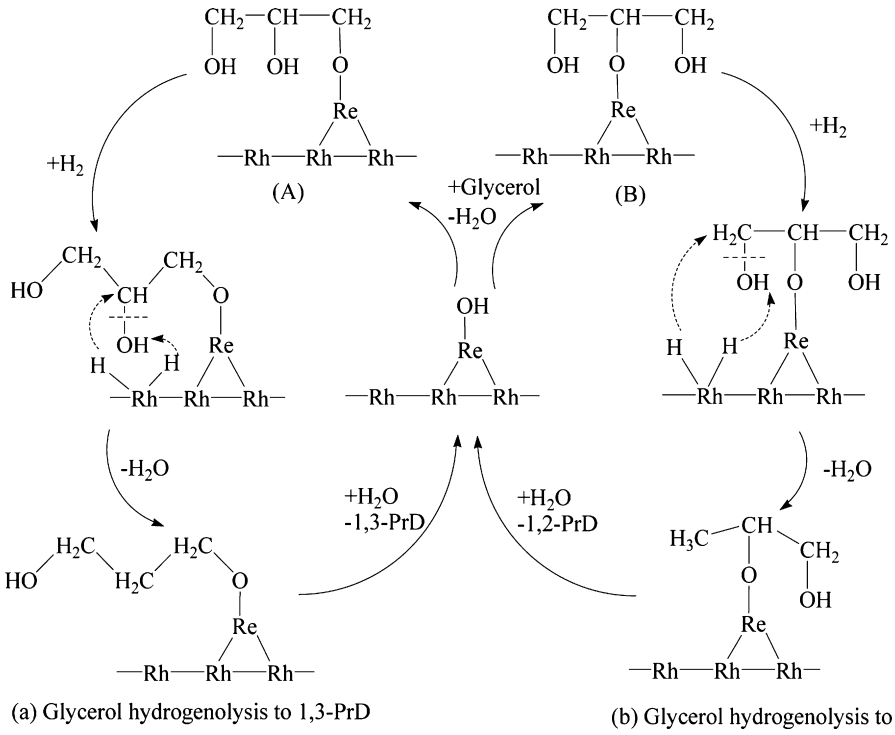

Fig. 14. A model scheme of glycerol hydrogenolysis to 1,3-PrD and 1,2-PrD on the interface between ReO_x and Rh metal surface over Rh-ReO_x/SiO_2.

state and this is also supported by the valence from Re L_3-edge XANES analysis (Fig. 11). The length of Re–O bond (0.210–0.211 nm) on Rh-ReO_x/SiO_2 (Re/Rh = 0.5) after the catalytic use and reduction was longer than that (0.174 nm) on NH_4ReO_4 and Rh-ReO_x/SiO_2 after the calcination, and the longer Re–O bond can be assigned to a single bond. The presence of Re-Rh bond demonstrates the direct interaction between Re species and Rh metal particles. The bond length of the Re–Rh bond (0.266–0.267 nm) on the catalyst after the reduction and the reaction was similar to that of Rh–Rh bond (0.268 nm) in Rh foil and the Re–Re bond (0.275 nm) in Re powder, and it was shorter than that of Rh–(O)–Rh bond (0.301 nm) in Rh_2O_3 [31,32]. This comparison indicates that the short Rh–Re bond is direct, and no oxygen atoms are located between Re species and Rh metal atoms. In addition, the bond formation can be related to small amount of CO adsorption of Rh-ReO_x/SiO_2 (Re/Rh = 0.5) considering that Rh metal particle sizes on Rh-ReO_x/SiO_2 (Re/Rh = 0.5) and Rh/SiO_2 were similar. This can be explained the partial covering of the surface Rh metal particles with reduced ReO_x species. Another important point is the presence of Re–Re bond. The bond length of the Re–Re bond (0.273–0.274 nm) on Rh-ReO_x/SiO_2 (Re/Rh = 0.5) was comparable to that of the Re–Re bond (0.274 nm) in the Re powder, and this indicates that no oxygen atoms are located between Re atoms. The coordination number (*CN*) (3.5) of the Re–Rh bond can be explained by the adsorption of Re atoms at three-fold hollow site of (1 1 1) surface and/or at four-fold hollow site of (1 0 0) surface. The coordination number (*CN*) (2.8 and 2.6) of the Re–Re bond is due to clustering of adsorbed Re species on the surface of Rh metal particles. The structure of Rh-ReO_x is compared to core-shell one, where core and shell consist of Rh metal and ReO_x clusters, respectively. This structure is constructed during the reduction, and it is maintained during the reaction as indicated by the results that XANES and EXAFS after the reaction were similar to these after the reduction. The results of Rh *K*-edge EXAFS analysis are shown in Fig. 13 and Table 2, and the presence of the Rh–Re bond was detected (*CN* = 1.8). The interaction between ReO_x species and Rh surface is also verified from the side of Rh.

3.4. Promoting effect of ReO_x over Rh metal particles on the reaction mechanism

It has been reported that the hydrogenolysis of glycerol can consist of the dehydration of glycerol over acid catalysts and consecutive hydrogenation over metal catalysts [5,12,33,34]. In the case of this indirect hydrogenolysis, the acidity of the catalysts is very important. Therefore, we evaluated the acidity of the reduced Rh-ReO_x/SiO_2 using methyl acetate hydrolysis as a model reaction. In this experiment, the amount of proton in 6.2 mg Amberlyst was just the same as the amount of Re on the 150 mg Rh-ReO_x/SiO_2. The conversion of Rh-ReO_x/SiO_2 (Re/Rh = 0.5) and Amberlyst15 were

Table 2
Curve fitting results of Rh *K*-edge EXAFS of Rh-ReO_x/SiO_2 (Re/Rh = 0.5).

Catalyst	Pretreatment	Shells	*CN*[a]	*R* (10^{-1} nm)[b]	σ (10^{-1} nm)[c]	ΔE_0 (eV)[d]	R_f (%)[e]
Rh-ReO_x/SiO_2	Reduction	Rh-Re	1.8	2.65	0.077	−10.4	0.8
		Rh-Rh	10.1	2.67	0.074	−0.5	
	Catalytic use	Rh-Re	1.8	2.66	0.078	−8.7	0.1
		Rh-Rh	10.1	2.68	0.077	0.4	

[a] Coodination number.
[b] Bond distance.
[c] Debye–Waller factor.
[d] Difference in the origin of photoelectron energy between the reference and the sample.
[e] Residual factor. Rh: 4 wt%, Re/Rh = 0.5. Fourier filtering range: 0.153–0.304 nm.

3.6% and 7.1%, respectively. This result means that the acidity of the reduced Rh-ReO_x/SiO_2 (Re/Rh = 0.5) catalyst is weaker than that of the Amberlyst. We have already reported that additive effect of Amberlyst on Rh/SiO_2 in the glycerol hydrogenolysis [11], however, the additive effect was not so remarkable as the case of Re. Acetol, the dehydration product of glycerol, was not detected in the reaction mixture of the Rh-ReO_x/SiO_2-catalyzed hydrogenolysis of glycerol. It should be noted that the indirect hydrogenolysis hardly produces 1,3-propanediol because the intermediate for 1,3-propanediol (3-hydroxypropionaldehyde) is much less stable than that for 1,2-propanediol (acetol) [4,5]. These tendencies suggest the direct glycerol hydrogenolysis over Rh-ReO_x/SiO_2 catalyst.

Promoting effect of ReO_x cluster attached on the surface of Rh metal particles on the activity of glycerol hydrogenolysis and the selectivity to 1,3-PrD formation is discussed in terms of the reaction mechanism. Since it has been known that adsorbed methoxy species is formed by the interaction between methanol and Re species [24,35]. In addition, it has been reported that the interaction between the $-CH_2OH$ group is tetrahydrofurfuryl alcohol and the ReO_x species on Rh-ReO_x/SiO_2 played an important role on the hydrogenolysis reaction [24]. On the basis that the reaction rate of the glycerol hydrogenolysis was independent of the glycerol concentration (Fig. 3), the alkoxide formation can be favorable and the coverage can be close to the saturation level. At the same time, negative effect of solvents such as methanol, ethanol and 1-butanol, is explained by the competitive interaction with ReO_x of OH group in the reactant and the solvent. In the glycerol hydrogenolysis, the synergy between ReO_x and Rh can be important and it is thought that the interface between Rh metal surface and attached ReO_x cluster can be the active site. Fig. 14 shows model scheme of glycerol hydrogenolysis to 1,3-PrD and 1,2-PrD over Rh-ReO_x/SiO_2. The adsorption of glycerol can give two kinds of alkoxides (A) and (B). Hydrogen atoms adsorbed on Rh metal surface can attack the C–O bond neighboring to the carbon with the alkoxide formation, as a result, 1,3-PrD and 1,2-PrD are given. At present, the selectivity and yield of 1,3-PrD formation is not satisfactory. In order to enhance them, it seems to be important to make the adsorption state of (A) favorable.

4. Conclusions

Addition of Re, Mo and W to Rh/SiO_2 enhanced the conversion of the glycerol hydrogenolysis in water. In particular, the formation of 1,3-propanediol was promoted by the modification with Re.

Promoting effect of Re addition to Rh/SiO_2 was maximum when Re/Rh = 0.5, and the excess addition of Re decreased the catalytic performance. In contrast, the number of Rh surface atoms estimated by CO adsorption decreased monotonously with increasing the amount of Re addition. The synergy between Rh and Re species promoted the glycerol hydrogenolysis.

The Rh-ReO_x/SiO_2 (Re/Rh = 0.5) catalyst maintained high selectivity of glycerol hydrogenolysis to propanediols and suppressed the side reactions such as the C–C bond breaking and propanediol hydrogenolysis even under the low H_2 pressure and high reaction temperature, where Rh/SiO_2 showed high side-reaction selectivities.

Characterization results indicated that Re species is present as Re^{7+} on the calcined Rh-ReO_x/SiO_2 (Re/Rh = 0.5) catalyst and it is reduced to +2 to +2.5 and interacted directly with Rh metal surface by the H_2 reduction pretreatment. In particular, the EXAFS analysis suggests the structure of ReO_x clusters is attached to the surface of Rh metal particles.

Effect of the glycerol concentration in aqueous solution on the reaction rate of the glycerol hydrogenolysis over Rh-ReO_x/SiO_2 (Re/Rh = 0.5) represents the strong interaction between glycerol and the catalyst surface, and the formation of alkoxides on the Re species is suggested.

The synergistic effect in the glycerol hydrogenolysis can be explained by the hydrogenolysis of the Re alkoxide species with hydrogen atoms on Rh metal surface, which proceeds on the interface between Rh metal surface and attached ReO_x species.

Acknowledgments

This work was in part supported by World Premier International Research Center (WPI), Initiative on Materials Nanoarchitectonics, MEXT, and the Industrial Technology Research Grant Program (no. 08B40001c) of New Energy and Industrial Technology Development Organization (NEDO) of Japan. Authors appreciate Dr. Tokushi Kizuka for TEM observation of the catalyst.

References

[1] A. Corma, S. Iborra, A. Velty, Chem. Rev. 107 (2007) 2411–2502.
[2] P. Gallezot, Green Chem. 9 (2007) 295–302.
[3] M. Pagliaro, R. Ciriminna, H. Kimura, M. Rossi, C.D. Pina, Angew. Chem. Int. Ed. 46 (2007) 4434–4440.
[4] M.A. Dasari, P.P. Kiatsimkul, W.R. Sutterlin, G.J. Suppes, Appl. Catal. A: Gen. 281 (2005) 225–231.
[5] Y. Kusunoki, T. Miyazawa, K. Kunimori, K. Tomishige, Catal. Commun. 6 (2005) 645–649.
[6] R. Lin, H. Liu, J. Hao, K. Cheng, Biotechnol. Lett. 27 (2005) 1755–1759.
[7] T.M. Che, U.S. Patent, 4 642 394 (1987).
[8] J. Chaminand, L. Djakovitch, P. Gallezot, P. Marion, C. Pinel, C. Rosier, Green Chem. 6 (2004) 359–361.
[9] T. Kurosaka, H. Maruyama, I. Naribayashi, Y. Sasaki, Catal. Commun. 9 (2008) 1360–1363.
[10] L. Huang, Y. Zhu, H. Zheng, G. Ding, Y. Li, Catal. Lett. 131 (2009) 312–320.
[11] I. Furikado, T. Miyazawa, S. Koso, A. Shimao, K. Kunimori, K. Tomishige, Green Chem. 9 (2007) 582–588.
[12] T. Miyazawa, Y. Kusunoki, K. Kunimori, K. Tomishige, J. Catal. 240 (2006) 213–221.
[13] S.R. Sashital, J.B. Cohen, R.L. Burwell Jr., J.B. Butt, J. Catal. 50 (1977) 479–493.
[14] Y.G. Chen, K. Tomishige, K. Yokoyama, K. Fujimoto, J. Catal. 184 (1999) 479–490.
[15] J.W. Cook, D.E. Sayers, J. Appl. Phys. 52 (1981) 5024–5031.
[16] K. Okumura, J. Amano, N. Yasunobu, M. Niwa, J. Phys. Chem. B 104 (2000) 1050–1057.
[17] K. Okumura, S. Matsumoto, N. Nishiaki, M. Niwa, Appl. Catal. B: Environ. 40 (2003) 151–159.
[18] A.L. Ankudinov, B. Ravel, J.J. Rehr, S.D. Conradson, Phys. Rev. B 58 (1998) 7565–7576.
[19] K. Tomishige, K. Asakura, Y. Iwasawa, J. Catal. 149 (1994) 70–80.
[20] T. Kubota, K. Asakura, N. Ichikuni, Y. Iwasawa, Chem. Phys. Lett. 256 (1996) 445–448.
[21] T. Kubota, K. Asakura, Y. Iwasawa, Catal. Lett. 46 (1997) 141–144.
[22] A.N. Mansour, J.W. Cook Jr., D.E. Sayers, J. Phys. Chem. 88 (1984) 2330–2334.
[23] J.A. Horsely, J. Chem. Phys. 76 (1982) 1451–1458.
[24] S. Koso, I. Furikado, A. Shimao, T. Miyazawa, K. Kunimori, K. Tomishige, Chem. Commn. (2009) 2035–2037.
[25] S. Koso, N. Ueda, Y. Shinmi, K. Okumura, T. Kizuka, K. Tomishige, J. Catal. 267 (2009) 89–92.
[26] A. Shimao, S. Koso, N. Ueda, Y. Shinmi, I. Furikado, K. Tomishige, Chem. Lett. 38 (2009) 540–541.
[27] L. Ma, D. He, Z. Li, Catal. Commun. 9 (2008) 2489–2495.
[28] L. Ma, D. He, Catal. Today (2009), doi:10.1016/j.cattod.2009.03.015.
[29] M. Rønning, T. Gjervan, R. Prestivik, D.G. Nicholson, A. Holmen, J. Catal. 204 (2001) 292–304.
[30] Y. Ishida, T. Ebashi, S. Ito, T. Kubota, K. Kunimori, K. Tomishige, Chem. Commn. (2009) 5308–5310.
[31] D.D. Beck, T.W. Capehart, C. Wong, D.N. Belton, J. Catal. 144 (1993) 311–324.
[32] T. Miyazawa, K. Okumura, K. Kunimori, K. Tomishige, J. Phys. Chem. C 112 (2008) 2574–2583.
[33] T. Miyazawa, S. Koso, K. Kunimori, K. Tomishige, Appl. Catal. A: Gen. 329 (2007) 30–35.
[34] T. Miyazawa, S. Koso, K. Kunimori, K. Tomishige, Appl. Catal. A: Gen. 318 (2007) 244–251.
[35] J. Liu, E. Zhan, W. Cai, J. Li, W. Shen, Catal. Lett. 120 (2008) 274–280.